

Supplementary Information for

Conformational Landscapes of Artificial Peptides Predicted by Various Force Fields: Are We Ready to Simulate β -Amino Acids?

Jihye Park,^a Hee-Seung Lee,^{a,b} Hyungjun Kim,^{a*} Jeong-Mo Choi^{c*}

^aDepartment of Chemistry, Korea Advanced Institute of Science and Technology (KAIST),
Yuseong-gu, Daejeon 34141, Republic of Korea

^bCenter for Multiscale Chiral Architectures, KAIST, Yuseong-gu, Daejeon 34141, Republic of
Korea

^cDepartment of Chemistry and Chemistry Institute for Functional Materials, Pusan National
University, Geumjeong-gu, Busan 46241, Republic of Korea

* Correspondence to: H. Kim (linus16@kaist.ac.kr) and J.-M. Choi (jmchoi@pusan.ac.kr)

This information supports the main manuscript and contains the following:

Table S1. The temperatures used for replica exchange molecular dynamics (REMD) simulations of the vacuum systems.....	4
Table S2. The temperatures used for REMD simulations of the methanol and water systems.....	4
Table S3. The p-value obtained by the t-test of $\phi - \theta$ distribution from hexamer simulations using different force fields and solvent conditions.....	5
Table S4. The p-value obtained by the t-test of $\psi - \theta$ distribution from hexamer simulations using different force fields and solvent conditions.....	6
Table S5. The average number of hydrogen bonds observed in vacuum, water, and methanol systems using different force field parameters.	7
Table S6. The multivariate linear regression result with the Pearson's R value, p -value, and fitting parameters C_1 , C_2 from the fitting model $y = C_1 \times N_{\text{intra-pep}} + C_2 \times N_{\text{sol-pep}} + K$	7
Table S7. The partial charges of the water (upper) and methanol (lower) molecules in the force fields used in this work.	8
Figure S1. The convergence test on the (a) PMF of ACPC monomer simulations with CHARMM36m force field, (b) PMF distribution of ACPC hexamer simulations with AMBER ff14SB force field in the aqueous system, and (c) ω distribution from aqueous systems. Overlap coefficients between the 15 ns, 20 ns, 30 ns, 40 ns, 50 ns, and 57 ns distribution were indicated as OC.....	10
Figure S2 Determination of the root-mean-squared deviation (RMSD) cutoff for clustering structures of ACPC monomer. We ran simulations for the vacuum system with (a) AMBER ff14SB, (b) CHARMM36m, and (c) OPLS-AA/L. The cutoff value of 0.5 Å is indicated with the dotted line.....	111
Figure S3. The RMSD of each structure to the average structure belongs to one cluster.	122
Figure S4. The probability distributions of the bootstrapped memory loss time (in ps). We ran simulations for four different solvent systems with AMBER ff14SB (left) and CHARMM36m (right): (a), (b) vacuum, (c), (d) water, (e), (f) methanol. The average and standard deviation are also shown.	133
Figure S5. The potential energies of dihedral angles ϕ (blue), θ (orange) and ψ (green) implemented in force fields (a) AMBER ff14SB, (b) CHARMM36m, and (c) OPLS-AA/L.....	144

Figure S6. RMSD values between the REMD sampled structure and DFT optimized global minimum structure for AMBER ff14SB (blue), CHARMM36m (orange), and OPLS-AA/L (green).	166
Figure S7. The distributions of average lengths of the helix pitch in the simulation data for the water system predicted by AMBER ff14SB (blue), CHARMM36m (orange), and OPLS-AA/L (green).	177
Figure S8. The example snapshot of a denatured helix observed in the aqueous system with OPLS-AA/L.	188
Figure S9. The $^3J_{\text{HN-H}\beta}$ coupling constant profile with corresponding ϕ angles	199
Figure S10. The multivariate linear regression results between intra-peptide, solvent-peptide hydrogen bond, and the ω from the (a, b) AMBER ff14SB, and (c, d) CHARMM36m force field in the water and methanol solvated systems.	20
Figure S11. Coulombic (Coul) interaction energies between cyclopentane (CP) side chain, amide backbone groups (BB), and solvents. (a) Comparison of Coulombic interaction energy from the methanol system with AMBER ff14SB (violet) and CHARMM36m (orange). (b) Comparison of Coulombic interaction energies from the aqueous system with AMBER ff14SB and CHARMM36m.	21

Table S1. The temperatures used for replica exchange molecular dynamics (REMD) simulations of the vacuum systems.

Temperature (K)									
300	310	325	350	375	400	425	450	475	500

Table S2. The temperatures used for REMD simulations of the methanol and water systems.

Temperature (K)									
300	305	310	315	320	325	330	335	340	345
350	355	360	365	370	375	380	385	390	395
400	405	410	415	420	425	430	435	440	445
450	455	460	465	470	475	480	485	490	495
500									

Table S3. The p-value obtained by the t-test of $\phi - \theta$ distribution from hexamer simulations using different force fields and solvent conditions.

	CHARM	OPLS-	AMBER	CHARM	OPLS-	AMBER	CHARM	OPLS-
$\phi - \theta$	M36m	AA/L	ff14SB	M36m	AA/L	ff14SB	M36m	AA/L
	vacuum	vacuum	methanol	methanol	methanol	water	water	water
AMBER ff14SB vacuum	0.097	0.097	0.347	0.101	0.266	0.045	0.088	0.422
CHARMM36m vacuum		0.088	0.069	0.272	0.128	0.031	0.129	0.089
OPLS-AA/L vacuum			0.094	0.099	0.188	0.147	0.098	0.273
AMBER ff14SB methanol				0.061	0.227	0.036	0.062	0.405
CHARMM36m methanol					0.125	0.019	0.178	0.092
OPLS-AA/L methanol						0.099	0.151	0.259
AMBER ff14SB water							0.017	0.195
CHARMM36m water								0.074

Table S4. The p-value obtained by the t-test of $\psi - \theta$ distribution from hexamer simulations using different force fields and solvent conditions.

	CHARM	OPLS-	AMBER	CHARM	OPLS-	AMBER	CHARM	OPLS-
$\psi - \theta$	M36m	AA/L	ff14SB	M36m	AA/L	ff14SB	M36m	AA/L
	vacuum	vacuum	Methanol	Methanol	Methanol	Water	Water	Water
AMBER ff14SB	0.131	0.137	0.172	0.135	0.105	0.038	0.110	0.109
vacuum								
CHARMM36m		0.163	0.175	0.140	0.126	0.108	0.126	0.107
vacuum								
OPLS-AA/L			0.152	0.168	0.193	0.206	0.184	0.132
vacuum								
AMBER ff14SB				0.112	0.155	0.055	0.068	0.074
Methanol								
CHARMM36m					0.246	0.127	0.362	0.189
Methanol								
OPLS-AA/L						0.190	0.242	0.177
Methanol								
AMBER ff14SB							0.117	0.237
Water								
CHARMM36m								0.227
Water								

Table S5. The average number of hydrogen bonds observed in vacuum, water, and methanol systems using different force field parameters.

System H-bonds type	Vacuum		Water		Methanol	
	$N_{\text{intra-pep}}$	$N_{\text{sol-pep}}$	$N_{\text{intra-pep}}$	$N_{\text{sol-pep}}$	$N_{\text{intra-pep}}$	$N_{\text{sol-pep}}$
AMBER ff14SB	2.00	X	0.97	4.68	1.39	3.83
CHARMM36m	0.88	X	0.60	3.97	0.86	2.50
OPLS-AA/L	0.97	X	0.01	7.35	0.80	0.01

Table S6. The multivariate linear regression result with the Pearson's R value, p -value, and fitting parameters C_1 , C_2 from the fitting model $y = C_1 \times N_{\text{intra-pep}} + C_2 \times N_{\text{sol-pep}} + K$.

Force Field	Solvent	R	p -value (K)	p -value (C_1)	p -value (C_2)	C_1	C_2
AMBER ff14SB	Methanol	0.314	0.000	2.32 $\times 10^{-55}$	9.48 $\times 10^{-52}$	2.746	-1.547
AMBER ff14SB	Water	0.175	0.000	3.36 $\times 10^{-26}$	2.50 $\times 10^{-10}$	2.651	-0.734
CHARMM 36m	Methanol	0.243	0.000	4.23 $\times 10^{-52}$	1.08 $\times 10^{-19}$	3.664	-1.263
CHARMM 36m	Water	0.113	0.000	1.09 $\times 10^{-10}$	1.58 $\times 10^{-6}$	1.625	-0.487

Table S7. The partial charges of the water (upper) and methanol (lower) molecules in the force fields used in this work.

Atom	TIP3P
O	-0.834
H	0.417

Atom	AMBER ff14SB	CHARMM36m	OPLS-AA/L
O	-0.5988	-0.650	-0.4826
H(O)	0.396	0.419	0.4057
C	0.1167	-0.039	0.1483
H(C)	0.0287	0.09	-0.0238

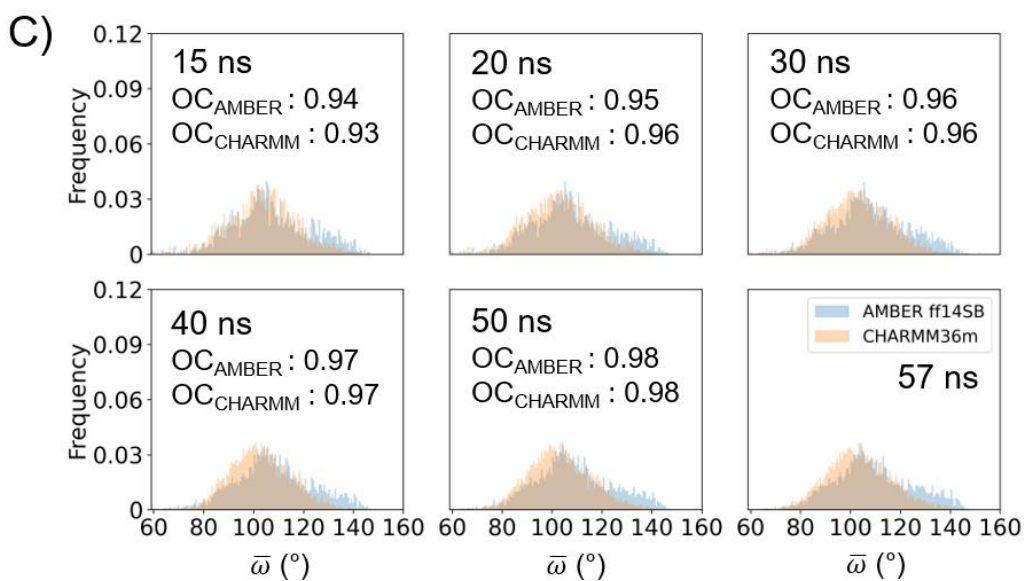
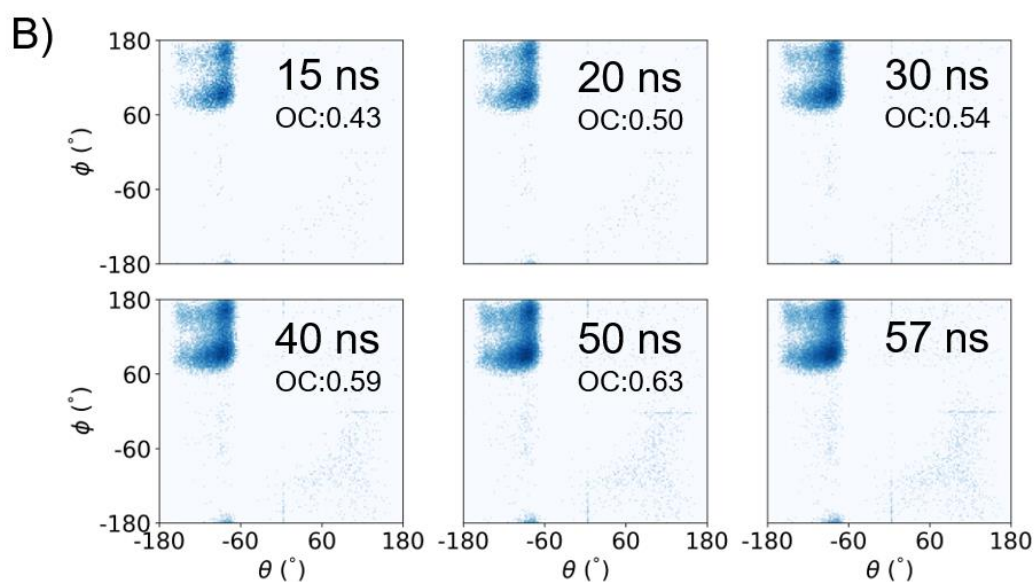
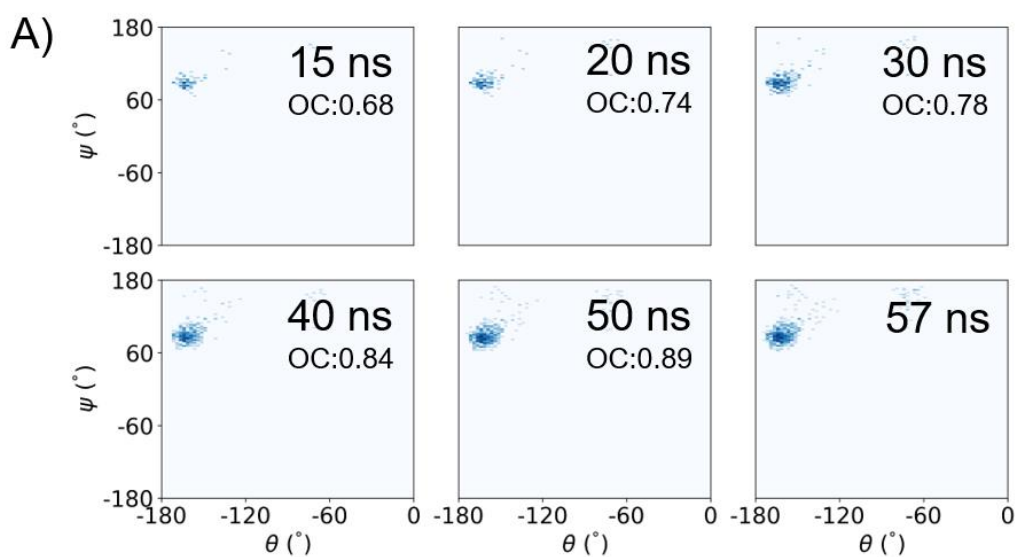


Figure S1. The convergence test on the (a) PMF of ACPC monomer simulations with CHARMM36m force field, (b) PMF distribution of ACPC hexamer simulations with AMBER ff14SB force field in the aqueous system, and (c) $\bar{\omega}$ distribution from aqueous systems. Overlap coefficients between the 15 ns, 20 ns, 30 ns, 40 ns, 50 ns, and 57 ns distribution were indicated as OC.

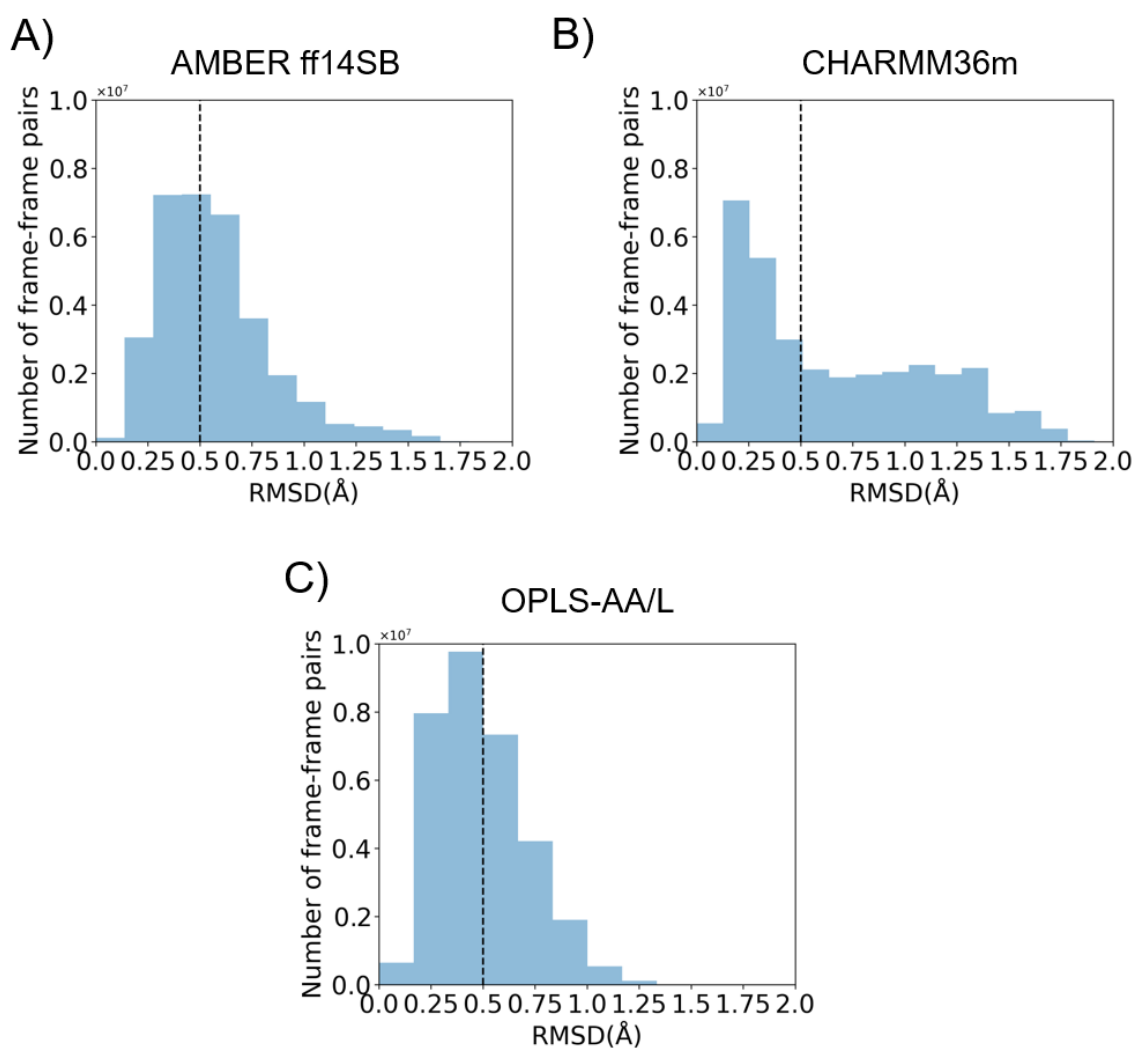


Figure S2. Determination of the root-mean-squared deviation (RMSD) cutoff for clustering structures of ACPC monomer. We ran simulations for the vacuum system with (a) AMBER ff14SB, (b) CHARMM36m, and (c) OPLS-AA/L. The cutoff value of 0.5 Å is indicated with the dotted line.

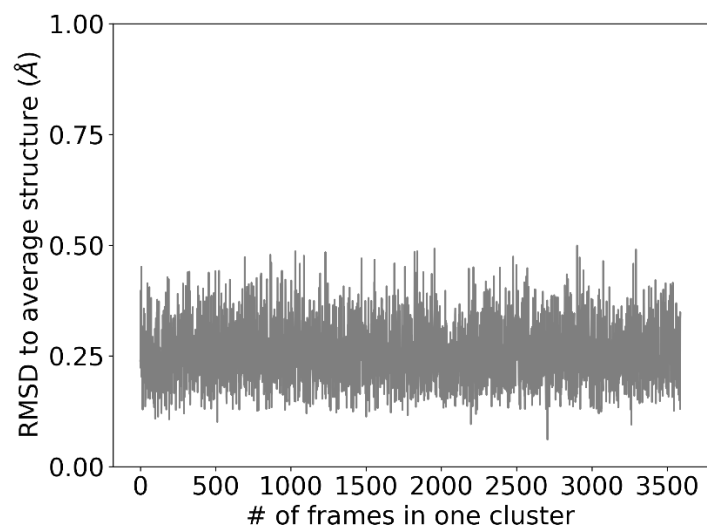


Figure S3. The RMSD of each structure to the average structure belongs to one cluster.

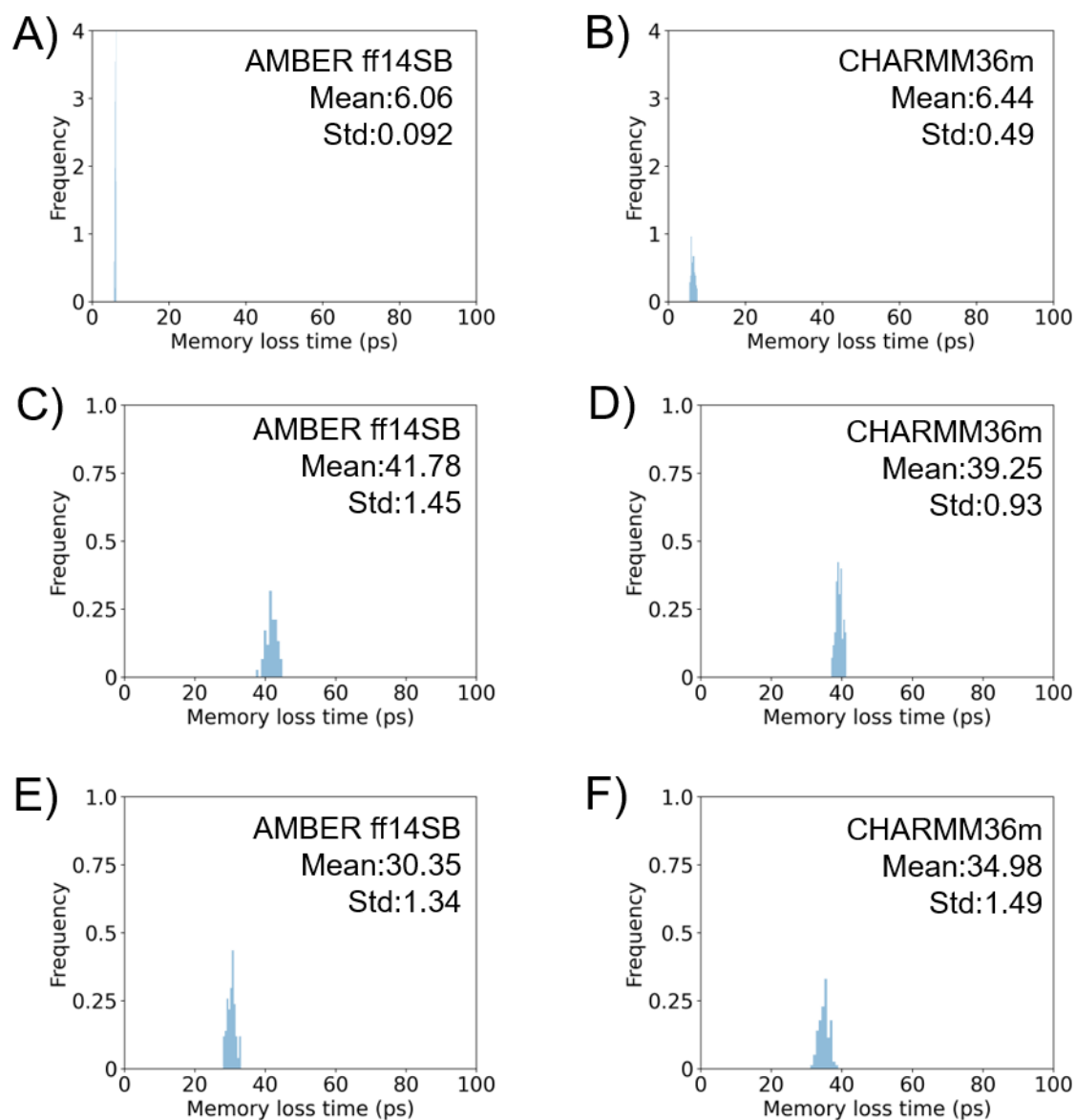


Figure S4. The probability distributions of the bootstrapped memory loss time (in ps). We ran simulations for four different solvent systems with AMBER ff14SB (left) and CHARMM36m (right): (a), (b) vacuum, (c), (d) water, (e), (f) methanol. The average and standard deviation are also shown.

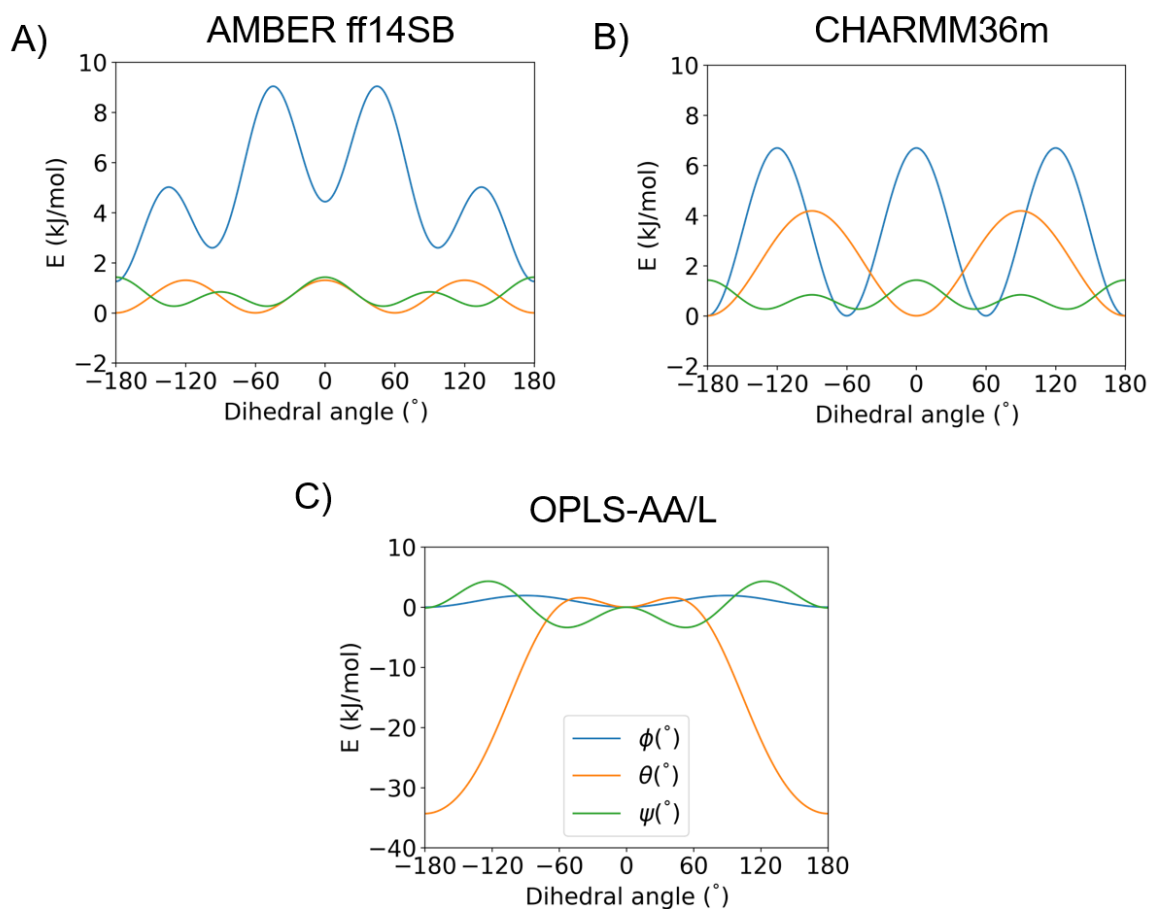


Figure S5. The potential energies of dihedral angles ϕ (blue), θ (orange) and ψ (green) implemented in force fields (a) AMBER ff14SB, (b) CHARMM36m, and (c) OPLS-AA/L.

The functional forms of dihedral potential energies from force field parameters are as following:

AMBER ff14SB:

$$E(\phi) = 2.21752(1 + \cos \phi) + 0.6276(1 + \cos(3\phi - 180)) + 2.092(1 + \cos(4\phi - 180))$$

$$E(\theta) = 0.650844(1 + \cos 3\theta)$$

$$E(\psi) = 0.29288(1 + \cos 2\psi) + 0.4184 (1 + \cos 4\psi)$$

CHARMM36m:

$$E(\phi) = 3.3472(1 + \cos 3\phi)$$

$$E(\theta) = 2.092(1 + \cos(2\theta - 180))$$

$$E(\psi) = 0.29288(1 + \cos 2\psi) + 0.4184 (1 + \cos 4\psi)$$

OPLS-AA/L:

$$E(\phi) = 1.93 - 1.933 \cos^2 \phi$$

$$E(\theta) = -8.79 + 23.849 \cos \theta - 8.368 \cos^2 \theta - 6.694 \cos^3 \theta$$

$$E(\psi) = 0.73 - 9.985 \cos \psi - 0.791 \cos^2 \psi + 10.042 \cos^3 \psi$$

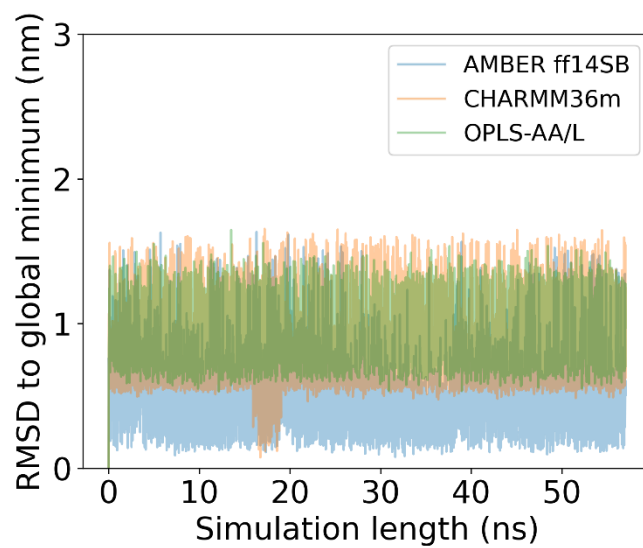


Figure S6. RMSD values between the REMD sampled structure and DFT optimized global minimum structure for AMBER ff14SB (blue), CHARMM36m (orange), and OPLS-AA/L (green).

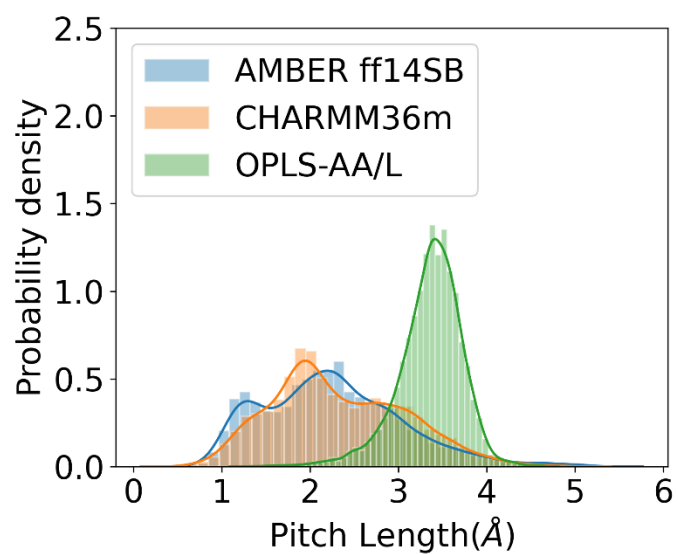


Figure S7. The distributions of average lengths of the helix pitch in the simulation data for the water system predicted by AMBER ff14SB (blue), CHARMM36m (orange), and OPLS-AA/L (green).

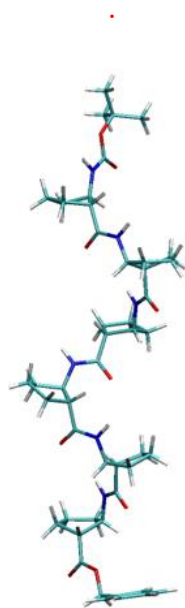


Figure S8. The example snapshot of a denatured helix observed in the aqueous system with OPLS-AA/L.

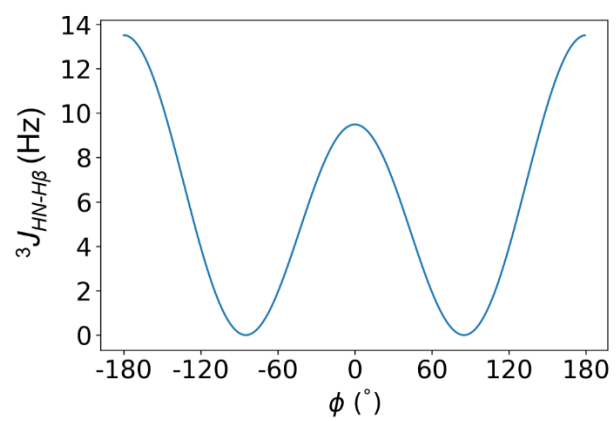
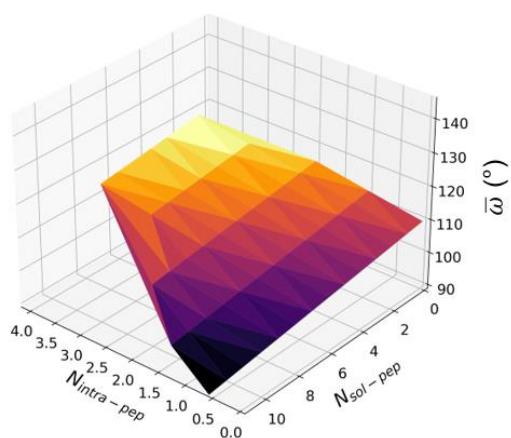
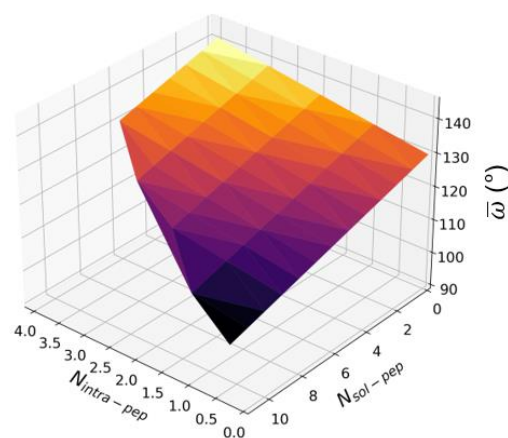


Figure S9. The ${}^3J_{\text{HN-H}\beta}$ coupling constant profile with corresponding ϕ angles

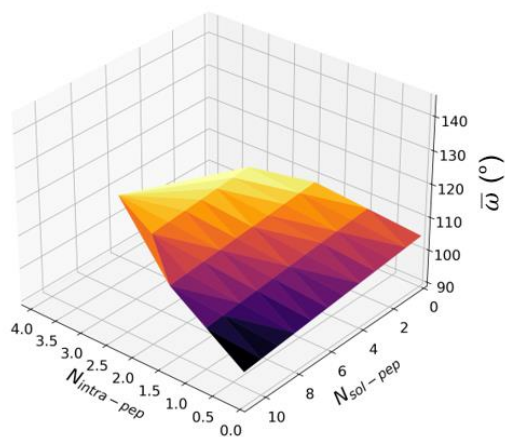
A) AMBER ff14SB Water



B) AMBER ff14SB Methanol



C) CHARMM36m Water



D) CHARMM36m Methanol

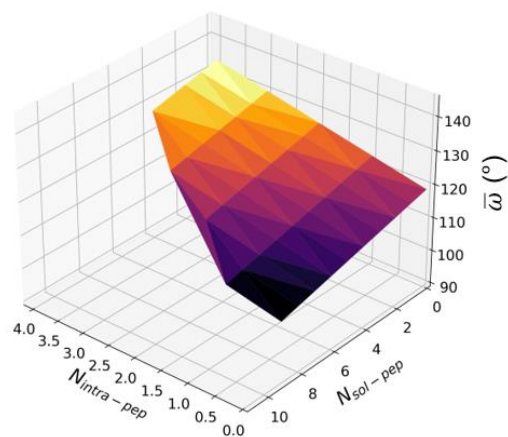


Figure S10. The multivariate linear regression results between intra-peptide, solvent-peptide hydrogen bond, and the $\bar{\omega}$ from the (a, b) AMBER ff14SB, and (c, d) CHARMM36m force field in the water and methanol solvated systems.

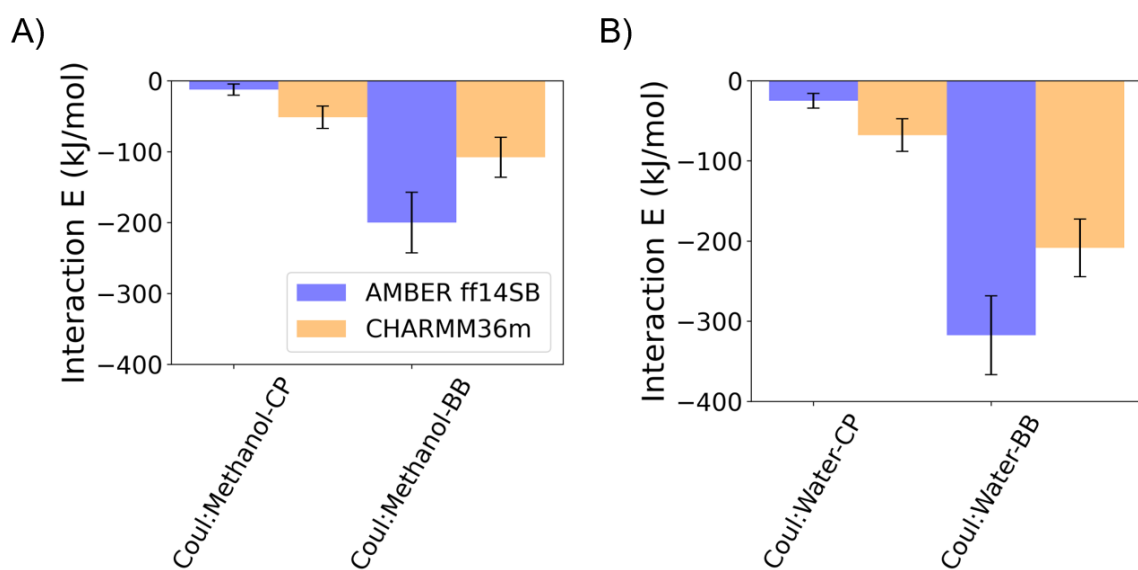


Figure S11. Coulombic (Coul) interaction energies between cyclopentane (CP) side chain, amide backbone groups (BB), and solvents. (a) Comparison of Coulombic interaction energy from the methanol system with AMBER ff14SB (violet) and CHARMM36m (orange). (b) Comparison of Coulombic interaction energies from the aqueous system with AMBER ff14SB and CHARMM36m.